A.N. WIECZOREK*#, D. MYSZKA**

ABRASIVE WEAR PROPERTIES OF Fe-BASED ALLOYS DESIGNED FOR MINING APPLICATIONS

The purpose of this study was to determine experimentally the wear properties of 5 groups of iron-based alloys used in the mining and transport machines exposed to the action of a hard abrasive material. The groups of materials to be examined included austempered ductile irons (ADI), steels and cast steel designed for quenching and tempering and for surface hardening, hard-wearing hardened steels and structural steels. The wear tests were carried out on a disc-on-disc test rig. The test samples were examined under conditions of sliding mating, while the leading destructive process was microcutting of the surface with loose corundum grain. The loss of mass of the examined samples was measured as a parameter characterizing the wear. Base on it, other wear coefficients were determined, for example the volume loss, the intensity of wear and the wear rate. The volume loss values determined were presented as a function of the strength and the initial hardness. Based on the results obtained, it was found that the hardened steel and ADI had comparable wear properties, while the ADI surface was strengthened probably as a result of the transition of austenite into martensite and the impact of the deformation of the graphite contained in ADI on the abrasive wear of the surface.

Keywords: wear, abrasion, ADI, steel, cast steel

1. Introduction

Ensuring an adequate level of reliability of the machines and equipment operated [1] is a fundamental problem of many industries. This problem is particularly important in the case of the operation of mining machines and equipment [2] working in the conditions where surface wear intensification factors occur. Hence there is a need to search for new applications for materials characterized by a high resistance to the abrasive wear. A reduction in the wear of machines is very important, bearing in mind also the respect for raw material reserves [3,4].

This paper presents results of tests of wear properties of the steels and cast steels commonly used in the mining industry as well as austempered ductile irons – ADI that may find many applications in the future. The study examines 5 groups of iron alloys that have a very significant share among all the materials used in mining machines. From this point of view, a comparison of the wear properties may allow selecting them in a more appropriate manner in order to ensure a lower wear of components of mining machines.

Advantageous performance characteristics of ADI are observed after properly conducted heat treatment that consists of austenitization and isothermal quenching. The conditions of the austenitization process determine the content of carbon in austenite, while the parameters of the "process window" of the isothermal transition shape ultimately the ausferritic microstruc-ture composed of bainitic ferrite and austenite. The combination of parameters of the isothermal transition temperature and the process duration is important for the diffusion of carbon into austenite and its further stabilization.

A characteristic feature of ADIs is the ability of strengthening as a result of the phase transition of austenite into strain-induced martensite caused by an increase in the stress or strain. A number of authors, including Schissler et al. [5], Owhadi et al. [6], Hayrynen et al. [7,8], Myszka and Wieczorek [9,10] confirmed a beneficial influence of the strain-induced transition on the wear properties of ADIs.

The heat treatment applied significantly increased the strength and plastic properties as compared with nodular cast irons. ADIs have the strength parameters comparable with those of alloy steels and cast steels used in machine components exposed to heavy loads. Therefore, the striving for replacing hard-wearing cast steels and forged alloy steels with ADIs has been observed for many years. Bahmani [11], Fordyce et al. [12], Kumari et al. [13], Perez et al. [14], Rundman et al. [15], Shepperson et al. [16], Zhou et al. [17] and Zimba et al. [18,19] found that ADIs had wear properties comparable with those of steels.

After quenching and tempering treatment, steels and cast steels are used in places where a high strength is needed, but they are not required to have a high wear resistance. However after surface hardening, the same steels and cast steels are character-

* SILESIAN UNIVERSITY OF TECHNOLOGY, FACULTY OF MINING AND GEOLOGY, 44-100 GLIWICE, POLAND
** WARSAW UNIVERSITY OF TECHNOLOGY, FACULTY OF PRODUCTION ENGINEERING, WARSAW, POLAND

Corresponding author: andrzej.n.wieczorek@polsl.pl

1522

ized by a good wear resistance and are used primarily for driving elements, such as chain wheels and gear wheels.

Hard-wearing steels became a standard in the mining industry and are used for elements that enable transport of excavated material from the mining site. Many manufacturers of steel offer materials of this type, but there are differences in wear properties of individual steels. Oyala et al. [20,21] examined 5 types of hard-wearing steels with nominally identical hardness and found significant differences reaching up to 50%. The steel with an addition of boron and nickel showed particularly good properties. Based on their studies, they proved that when selecting the materials for elements exposed to wear not only the hardness, but first of all the chemical composition and the microstructure were important factors. Wear properties of the hard-wearing hardened steels were further analysed in [22,23].

Structural steels are used in construction of mining machines, primarily for supporting structures. They are not designed for operation in the conditions of an increased abrasive wear. However, as the mining practice shows, they are often exposed also to the action of an abrasive as a result of improper selection of material imposed by economic considerations. Therefore in the article presents a study on abrasive wear these popular modern steel and cast iron entering the market for mining machinery.

2. Experimental details

2.1. Characteristics of the materials tested

For the tests of wear properties, 16 material variants were used. They can be classified into the following groups of iron alloys:
– austempered ductile irons (6 variants),
– alloy steels and cast steels designed for quenching and tempering (3 variants) and surface hardening (3 variants),
– hard-wearing hardened steels (2 variants)
– rolled structural steels (2 variants).

Within the group of ADI, the following according to the PN-EN 1564:2012 [24] variants have been analysed:
– ADI_NiCu_370 that meets the requirements of the EN-GJS-800-8 grade,
– ADI_NiCu_330 that meets the requirements of the EN-GJS-1000-5 grade,
– ADI_NiCu_270 that meets the requirements of the EN-GJS-1200-2 grade,
– ADI_NiMo_370 that meets the requirements of the EN-GJS-800-8 grade,
– ADI_NiMo_320 that meets the requirements of the EN-GJS-1000-5 grade,
– ADI_NiMo_270 that meets the requirements of the EN-GJS-1200-2 grade.

Nodular cast irons of the EN-GJS-600-3 grade according to the PN-EN 1563 standard were used to produce the ADI_NiCu and ADI_NiMo series austempered ductile irons. Their chemical

compositions are shown in Table 1. The matrix of the nodular cast iron had a pearlitic-ferritic structure (a sample microstructure of the cast iron used to produce ADI_NiMo is shown in Fig. 2), where the number of graphite nodules per mm^2 was not less than 200 and the degree of spheroidization was greater than 90%. List of the process parameters is presented in Table 2, while Fig. 1 shows a diagram of the heat treatment of ADI.

TABLE 1

Chemical composition of 2 ductile irons EN-GJS-600 [mass%] for ADI_NiCu, ADI_NiMo variants

	C	Si	Mn	S	P
ADI_NiCu	3,60	2,45	0,32	0,04	0,035
	Mg	Cu	Ni	Mo	
	0,065	0,93	1,90	0,01	
ADI_NiMo	C	Si	Mn	S	P
	3,85	2,90	0,61	0,01	0,05
	Mg	Cu	Ni	Mo	
	0,08	0,02	1,50	0,47	

In the group of hard-wearing steels, two materials (the designations used in this study do not correspond to the actual trade names of the materials) with differentiated surface hardness were examined (the manufacturer of the materials did not disclose any details concerning the heat treatment):
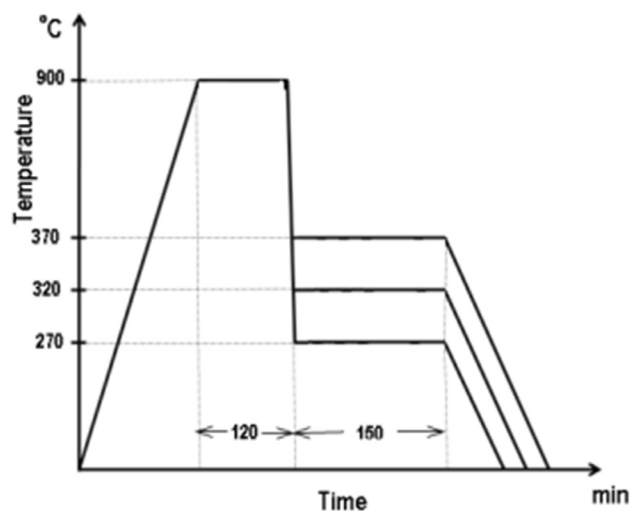– WRSteel_400,
– WRSteel_500.

Fig. 1. Diagram of the heat treatment process for the ADI tested

In the group of the alloy steels and cast steels subjected to quenching and tempering (Table 3), the following materials were examined:
– steel 34CrNiMo6 (Q+T),
– cast steel GS40CrMo4 (Q+T),
– cast steel L35HGS (Q+T).

The materials mentioned above were tested also in the quenched and tempered state (Table 3). They were designated as: 34CrNiMo6 (H), GS40CrMo4 (H), L35HGS (H).

The process parameters used for the production of ADI

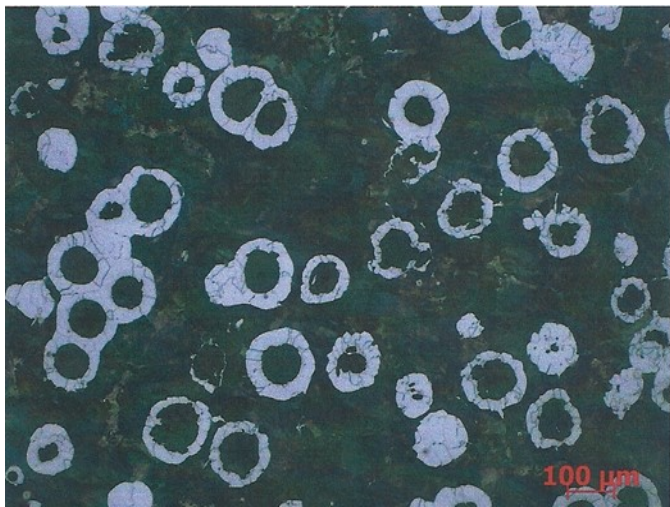| Heat treatment parameters	ADI_NiCu_270 ADI_NiMo_270	ADI_NiCu_320 ADI_NiMo_320	ADI_NiCu_370 ADI_NiMo_370
Austenitising temperature,°C	900		
Austenitising time, min	120		
Austempering temperature,°C	270	320	370
Austempering time, min	150		

Fig. 2. Initial structure ductile iron of the ADI_NiMo series

Two types of structural steels were also subjected to wear tests under the studies:

– the STEEL_700MC steel in the state after a thermomechanical treatment (own designation used for the needs of this study due to the use of a trade name by the manufacturer),

– the S355J2 steel in the normalized state (this steel was also selected as a reference material, in relation to which the wear resistance of other materials was compared).

Table 4 presents the determined values of the maximum strength TS for the materials examined and the measured value of the surface hardness H. The measurement uncertainty for both values was determined for the confidence level of 0.95 and the number of replications $n = 3$. The relative uncertainty of measurement was less than 5% for all the cases considered.

2.2. Test rig and methods

For testing the wear of the samples of the materials in question, a disc-on-disc test rig was used (Fig. 3A), which was described in detail in [25]. The main friction pair consists of two ring-shaped samples, between which an abrasive material is located. During the tests, corundum grains with a diameter

The process parameters used for the production of steel and cast steel samples

Heat treatment parameters	34CrNiMo6 (Q+T)	L35GSM (Q+T)	GS40CrMo4 (Q+T)
Austenitising temperature,°C	860		
Austenitising time, min	120		
Quenching temperature,°C	760		
Tempering temperature,°C	600		
Heat treatment parameters	34CrNiMo6 (H)	L35GSM (H)	GS40CrMo4 (H)
Austenitising temperature,°C	860		
Austenitising time, min	120		
Quenching temperature,°C	760		
Tempering temperature,°C	180		

Mechanical properties of the steels, cast steels and ADI tested

Material	Tensile Strength TS, MPa	Hardness H, HRC
ADI_NiCu_370	944	31
ADI_NiCu_330	1140	37
ADI_NiCu_270	1457	45
ADI_NiMo_370	872	30
ADI_NiMo_330	1159	37
ADI_NiMo_270	1270	44
34CrNiMo6 (H)	1030	56
34CrNiMo6 (Q+T)		34
L35HGS (H)	1100	54
L35HGS (Q+T)		29
GS40CrMo4 (H)	75	56
GS40CrMo4 (Q+T)		29
WRSteel_400	1250	43
WRSteel_500	1600	51
STEEL_700MC	850	23
S355J2	520	21

below 50 μm were used as the abrasive. They were added in an amount of 1 cm³ between mating samples (Fig. 3B).

A characteristic feature of the test conducted at this test rig is a constant presence of the abrasive between the samples as well as the presence of crushed grains and wear products originating from the damaged surface. This situation corresponds with many cases of the actual wear of machine components. When conducting the tests, an observation was made that corundum grains were completely crushed in the maximum time up to 10 minutes.

The research methodology assumed that after each 10-minute wear cycle the samples will be cleaned and weighed and fresh corundum abrasive will be added. The basic parameters

characterizing the wear test are presented in Table 5. The wear parameter to be determined was defined by the formula (1):
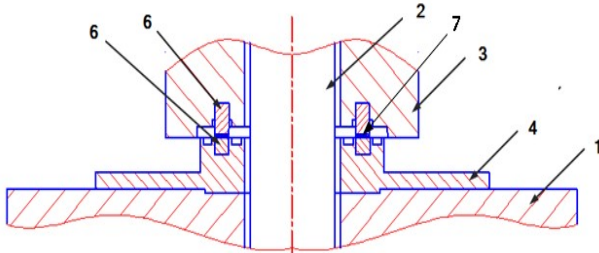
$$u_M = \left(m_{pd0} - m_{pdt}\right) + \left(m_{pg0} - m_{pgt}\right) \qquad (1)$$

where:

m_{pd0} – mass of the lower sample before starting the test, g,
m_{pdt} – final mass of the lower sample, g,
m_{pg0} – mass of the upper sample before starting the test, g,
m_{pgt} – final mass of the upper sample, g
u – loss of the mass of samples, g.
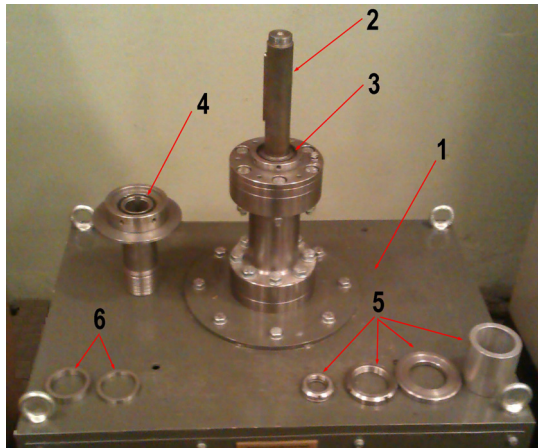
A

B

Fig. 3. The design of the IMG stand; A – View of the test rig, B – Diagram of sample fixing, 1 – body of the test rig with a motor, 2 – drive shaft, 3 – upper sample holder, 4 – lower sample holder, 5 – fastening elements, 6 – test samples, 7 – abrasive

Volumetric wear u_v was determined using the relationship (2):

$$u_v = \frac{u_M}{\rho} \qquad (2)$$

where: ρ – mass density, g/mm^3.

TABLE 5

Basic parameters of the wear tests

Unit preasure σ, MPa	0,031	0,062	0,094	0,125
Peripheral speed v, m/s	0,29			
Time of testing, min	8×10			
Friction distance, m	1520			

Wear intensity I_H was determined using the relationship (3):

$$I_H = \frac{u_L}{s} = \frac{\left(\dfrac{u_v}{A}\right)}{s} \qquad (3)$$

where:

u_L – linear wear, mm,
s – friction path, m,
A – nominal sample contact area, mm^2.

The wear rate parameter determines the linear wear in a given unit of time (a commonly used unit, i.e. μm/h, was accepted for the needs of this study). Parameter s_v is determined by the formula (4):

$$s_v = v_s \cdot I_H \qquad (4)$$

where: v_s – sliding velocity, m/s.

The uncertainty of the determination of the mass wear was specified for the confidence level of 0.95 and the number of replications $n = 3$. The relative uncertainty of measurement was less than 3% for all the cases considered.

3. Results

The microcutting with the loose abrasive of a significant hardness was the process responsible for destroying the surface of the contact zone. During the wear tests three stages of the surface destruction in the test samples were distinguished:

– microcutting with uncrushed corundum abrasive grains,
– mutual crushing of abrasive grains caused by their movement,
– cutting with crushed abrasive of superfinish character.

An example of traces of surface damage to ADI_NiMo series cast iron and hardened steels, caused by corundum abrasive, are shown in Fig. 4.

In Fig. 4 there are clearly visible scratches running in the direction consistent with the movement of corundum grain between the samples. The depth and extent of damage to the surface varied depending on the iron alloy tested. The deepest scratches was found in the case of structural steels and toughened steels.

The scratches presented in Fig. 4 were most likely formed in the initial stage of the surface destruction. Visible superfinishing zones could have been formed as a result of the action of the crushed abrasive.

The values calculated with the use of the formula (1) provided a basis for determining the total mass wear $u_{M\Sigma}$ after the entire duration of the test (Table 6).

Using the formulas (2), (3) and (4), the total volumetric wear $u_{v\Sigma}$ (Table 7), the wear intensity I_H (Table 8) and the wear rate s_v (Table 9) were determined too.

Values of the total volumetric wear $u_{M\Sigma}$ are presented as a function of the maximum strength (Fig. 5) and the initial hardness (Fig. 6) in a breakdown into 5 groups of iron alloys: austempered ductile irons, alloy steels and cast steels after quenching and tempering, alloy steels and cast steels after hardening and
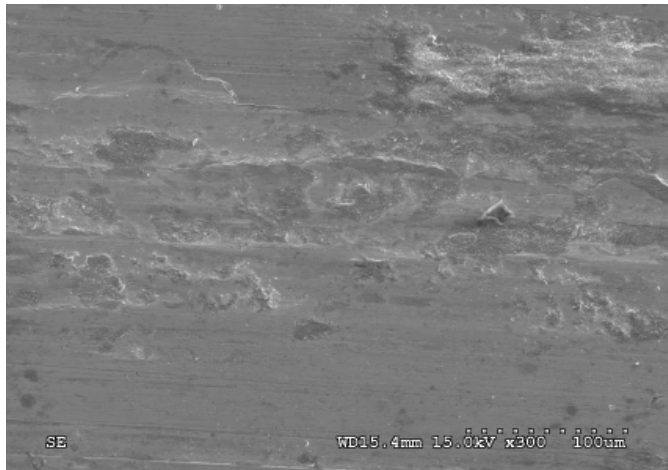
L35GSM (H)

ADI_NiMo_330

Fig. 4. Abrasive wear of L35GSM cast steel and ADI_NiMo_330 (SEM)

low-temperature tempering, hardened hard-wearing steels, and rolled structural steels.

Fig. 7 shows the values of the Relative Wear Resistance (RWR) coefficient [27] determined with the use of the relationship (5):

$$RWR = \frac{\text{Weight loss of sample S355J2}}{\text{Weight loss of sample}} \quad (5)$$

The *RWR* coefficient determines the multiplication of the total mass wear $u_{M\Sigma}$ of the analysed material in relation to the S355J2 structural steel. The S355J2 steel was selected due to its prevalence in machine building. Values of the *RWR* coefficient for ADI are in the range from 3.8 to 14.5, while for steels and quenched and tempered cast steels they range between 2.6 and 10.2.

Based on the results presented in Tables 6 to 10 and their graphical presentation in Figs. 5-7, it is easy to notice that ADI are characterised by similar or more favourable wear properties as compared with hardened steels and cast steels designed for use in harsh operating conditions. As compared with quenched and tempered steels and cast steels as well as structural steels, ADI are characterized by much more favourable wear properties.

TABLE 6

Values of the total mass wear $u_{M\Sigma}$ for all the materials examined

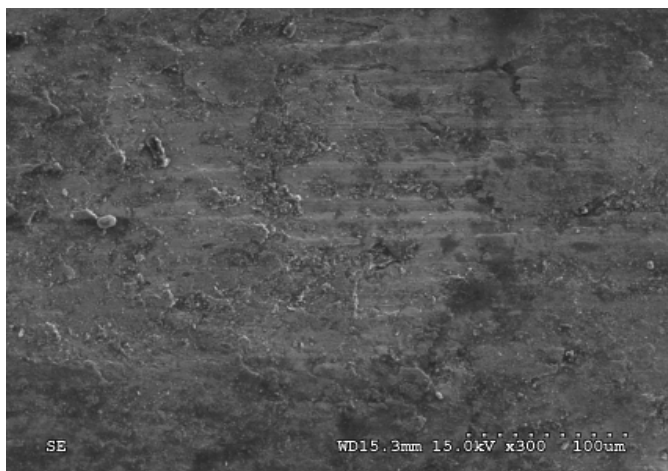| $u_{M\Sigma}$, g	0,031 MPa	0,062 MPa	0,094 MPa	0,125 MPa
ADI_NiCu_370	0,272	0,291	0,324	0,335
ADI_NiCu_330	0,400	0,393	0,334	0,306
ADI_NiCu_270	0,423	0,443	0,482	0,538
ADI_NiMo_370	—	0,564	0,490	0,796
ADI_NiMo_330	—	0,459	0,350	0,452
ADI_NiMo_270	—	0,241	0,348	0,335
34CrNiMo6 (H)	0,341	0,341	0,592	0,592
34CrNiMo6 (Q+T)	2,664	3,320	3,720	3,810
L35HGS (H)	0,458	0,458	0,663	1,264
L35HGS (Q+T)	1,742	1,773	1,972	2,157
GS40CrMo4 (H)	1,053	1,259	1,228	1,263
GS40CrMo4 (Q+T)	1,016	1,570	1,848	1,952
WRSteel_400	0,899	1,157	1,559	—
WRSteel_500	0,877	1,195	1,296	—
STEEL_700MC	2,924	3,257	3,797	—
S355J2	3,485	3,485	4,041	—

TABLE 7

Values of the total volumetric wear $u_{v\Sigma}$ for all the materials examined

$u_{v\Sigma}$, mm^3	0,031 MPa	0,062 MPa	0,094 MPa	0,125 MPa
ADI_NiCu_370	37,46	40,08	44,72	46,22
ADI_NiCu_330	55,10	54,21	46,08	42,19
ADI_NiCu_270	58,32	61,08	66,44	74,25
ADI_NiMo_370		77,78	67,63	109,79
ADI_NiMo_330		63,34	48,21	62,34
ADI_NiMo_270		33,20	48,06	46,15
34CrNiMo6 (H)	43,11	43,11	74,90	74,90
34CrNiMo6 (Q+T)	337,17	420,19	470,86	482,25
L35HGS (H)	57,97	57,97	83,97	159,99
L35HGS (Q+T)	220,52	224,42	249,62	273,00
GS40CrMo4 (H)	133,24	159,33	155,46	159,84
GS40CrMo4 (Q+T)	128,66	198,68	233,90	247,13
WRSteel_400	113,84	146,40	197,28	—
WRSteel_500	111,06	151,29	164,01	—
STEEL_700MC	370,13	412,22	480,69	—
S355J2	441,15	441,15	511,48	—

The observations of the microstructure were performed using a metallographic optical microscope with 50×-1000× magnification. The samples were ground, polished and etched with 2% Nital solution.

Fig. 8 shows the microstructure of the ADI_NiMo series ductile iron, while Fig. 9 presents the microstructure of the ADI_NiCu series ductile iron. The ADI_NiMo_370 and ADI_NiCu_370 cast irons have a structure of upper ausferrite containing bainitic ferrite and austenite, the overall content of which was estimated at a level of approx. 40%.

Values of the wear intensity I_H for all the materials examined

I_H, 10^{-6}	0,031 MPa	0,062 MPa	0,094 MPa	0,125 MPa
ADI_NiCu_370	0,029	0,031	0,034	0,036
ADI_NiCu_330	0,042	0,042	0,035	0,032
ADI_NiCu_270	0,045	0,047	0,051	0,057
ADI_NiMo_370	—	0,060	0,052	0,084
ADI_NiMo_330	—	0,049	0,037	0,048
ADI_NiMo_270	—	0,026	0,037	0,035
34CrNiMo6 (H)	0,036	0,036	0,063	0,063
34CrNiMo6 (Q+T)	0,282	0,352	0,394	0,404
L35HGS (H)	0,049	0,049	0,070	0,134
L35HGS (Q+T)	0,185	0,188	0,209	0,229
GS40CrMo4 (H)	0,112	0,133	0,130	0,134
GS40CrMo4 (Q+T)	0,108	0,166	0,196	0,207
WRSteel_400	0,095	0,123	0,165	—
WRSteel_500	0,093	0,127	0,137	—
STEEL_700MC	0,310	0,345	0,403	—
S355J2	0,369	0,369	0,428	—

Values of the wear rate s_v for all the materials examined

s_v, µm/h	0,031 MPa	0,062 MPa	0,094 MPa	0,125 MPa
ADI_NiCu_370	30,06	32,16	35,88	37,08
ADI_NiCu_330	44,21	43,49	36,97	33,85
ADI_NiCu_270	46,79	49,00	53,30	59,57
ADI_NiMo_370	—	62,40	54,26	88,08
ADI_NiMo_330	—	50,81	38,68	50,02
ADI_NiMo_270	—	26,64	38,55	37,03
34CrNiMo6 (H)	37,69	37,69	65,48	65,48
34CrNiMo6 (Q+T)	294,76	367,33	411,63	421,59
L35HGS (H)	50,68	50,68	73,41	139,86
L35HGS (Q+T)	192,78	196,19	218,22	238,66
GS40CrMo4 (H)	116,48	139,29	135,90	139,73
GS40CrMo4 (Q+T)	112,47	173,69	204,48	216,04
WRSteel_400	99,52	127,98	172,46	—
WRSteel_500	97,09	132,26	143,38	—
STEEL_700MC	323,57	360,37	420,22	—
S355J2	385,66	385,66	447,14	—

In the case of the ADI_NiMo_320 and ADI_NiCu_320 cast irons, upper ausferrite was also found, but with a lower content of austenite (approx. 28%). The ADI quenched isothermally at the lowest temperature (ADI_NiMo_270 and ADI_NiCu_270) have the structure of lower ausferrite with the content of austenite below 20%.

Fig. 10 shows the structure of hardened steels and cast steels. The surface layer of the 34CrNiMo6 steel has a uniform structure of tempered martensite with a small amount of residual austenite. The GS40CrMo4 cast steel is characterized by a heterogeneous microstructure composed of a thin layer (approx. 0.02 mm) of martensite tempered with austenite and the underlying mix of sorbite, residual austenite and single inclusions of bainite. The microstructure of the L35HGS cast steel consists of tempered martensite with quite numerous inclusions of bainite. The 34CrNiMo6 steel as well as the L35HGS and GS40CrMo4 L35HGS cast steels in the quenched and tempered state have a sorbitic structure. Fig. 11 shows the microstructure of the WRS_400 and WRS_500 hard-wearing steels, Fig. 12 presents the microstructure of the STEEL_700MC steel, while Fig. 13 – the microstructure of the S355J2 steel.

For both WRS_400 and WRS_500 hard-wearing steels, the predominant phase of the microstructure is martensite. In addition there occurs also residual austenite. In the case of steels with a higher hardness (WRS_500), the share of austenite is lower.

The structure of the STEEL_700MC steel consists of a mix of fragmented ferrite and pearlite. The grains are characterised by a deformation associated with the process of thermomechanical treatment. The S355J2 steel is composed also of ferrite and pearlite, however the predominance of the first phase is observed. The microstructure is characterized by distinct grain banding and deformation resulting from the rolling process.

4. Discussion

The ADI showed very advantageous wear properties in the presence of the corundum abrasive as compared with other types of materials under consideration. The reason of a high wear resistance is most likely the transition of austenite into martensite occurring in the surface layer under a load. The authors analysed the problem of the phase transitions occurring in cast irons containing Ni and Cu in their earlier study [9]. They found, inter alia, a distinct correlation between the content of metastable austenite and an increase in the surface hardness.

A relationship between the difference in the hardness of the operating surface layer and the core was also observed in this study (designation Delta_H in Fig. 14). For ADI of the ADI_NiCu and ADI_NiMo series, a linear dependence between this increase and the isothermal quenching temperature was presented (Fig. 14). The strengthening of the surface is comparable for both ADI series.

However, when analysing the value of wear as a function of isothermal quenching temperature (Fig. 15), two different trends can be observed. For ADI of the ADI_NiCu series, the wear increases along with an increase in the isothermal quenching temperature, while for ADI of the ADI_NiMo series the dependence is inverse.

In the case of ADI containing Ni and Cu, the dependence established coincides with the results obtained in other studies. PourAsiabi et al. [27], after conducting pin-on-disc tests, found that the wear increased along with an increase in the isothermal quenching temperature. The authors found that the most optimal time of the isothermal transition that ensured the highest wear
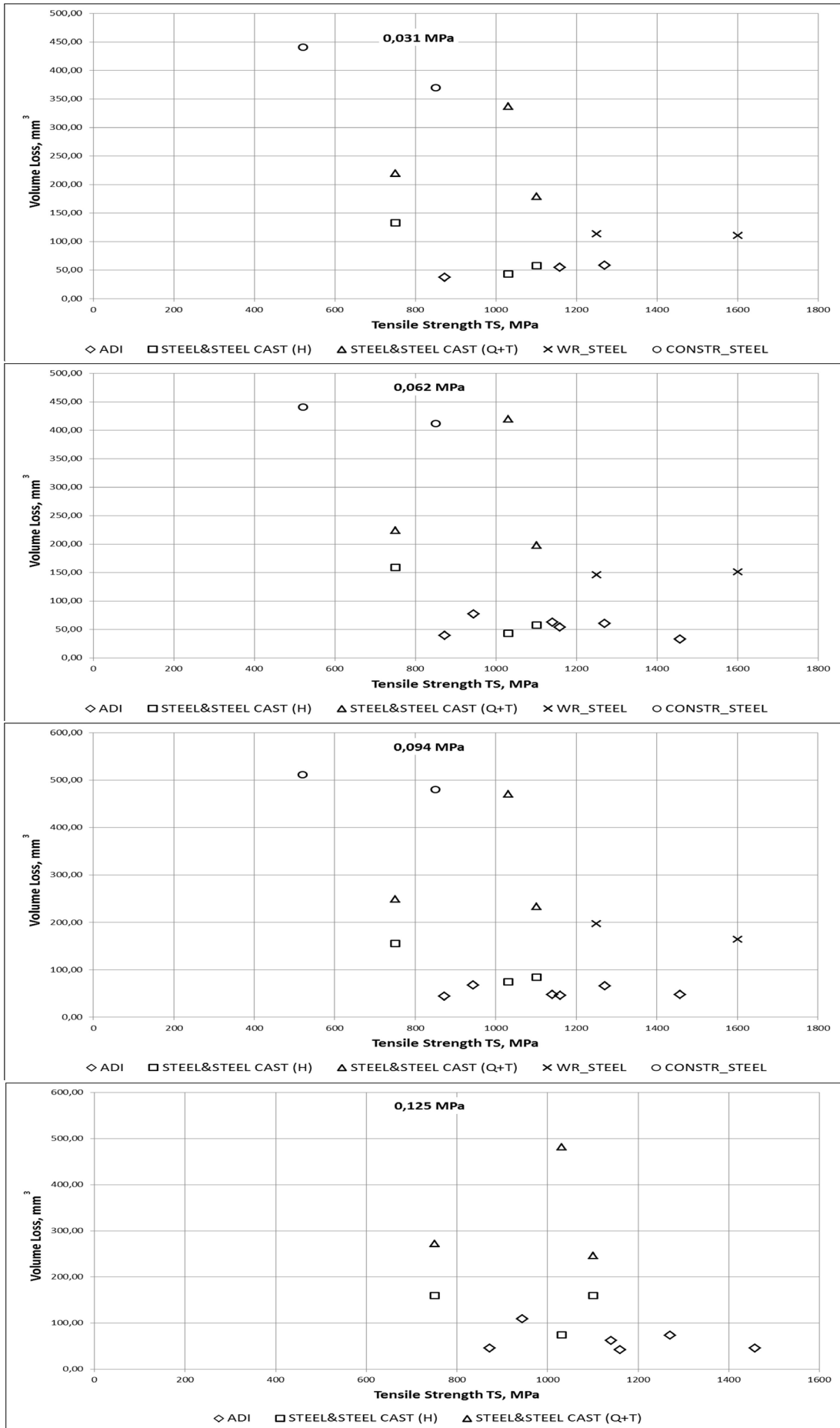
Fig. 5. Values of the total volumetric wear $u_{v\Sigma}$ as a function of the Tensile Strength TS
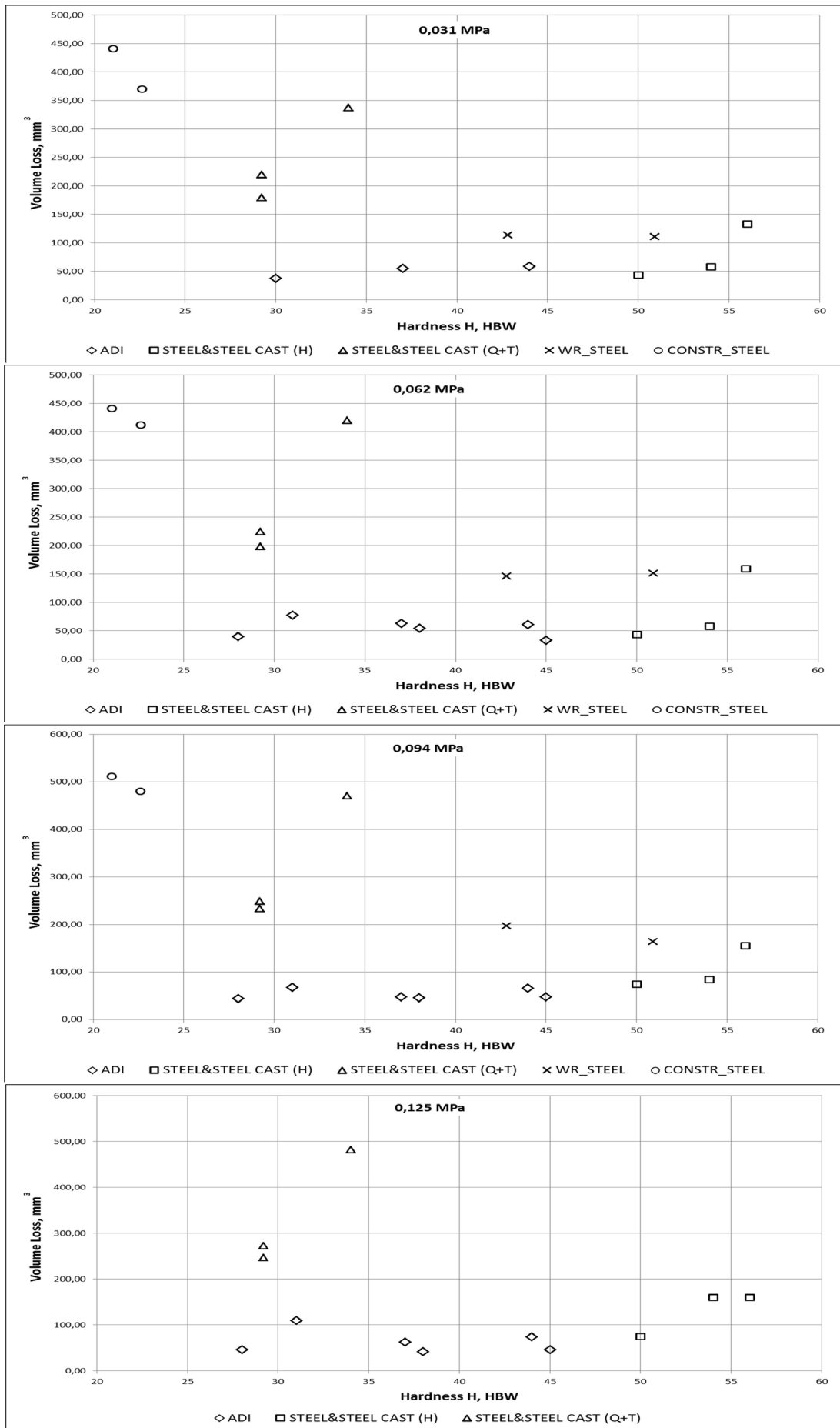
1528

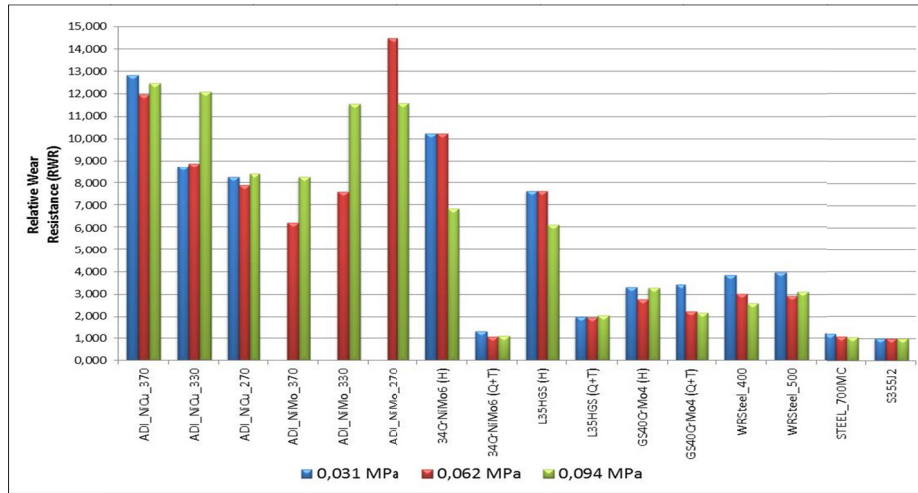Fig. 6. Values of the total volumetric wear $uv\Sigma$ as a function of the initial hardness H

Fig. 7. Values of the Relative Wear Resistance (*RWR*) coefficient determined for the materials examined
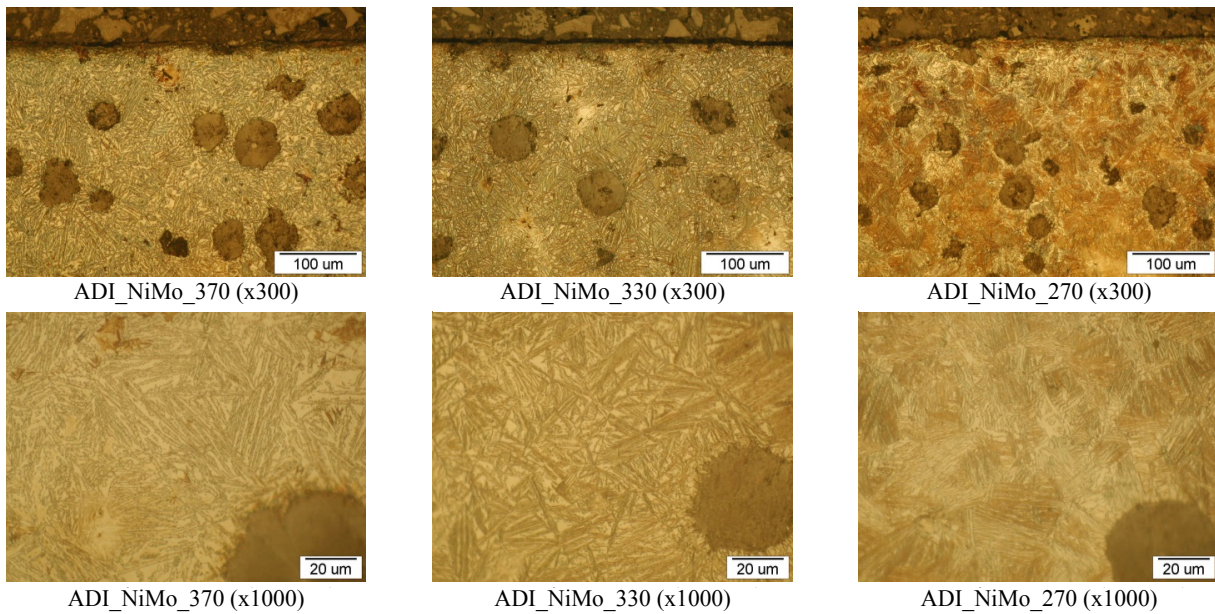

ADI_NiMo_370 (x300) · ADI_NiMo_330 (x300) · ADI_NiMo_270 (x300)

ADI_NiMo_370 (x1000) · ADI_NiMo_330 (x1000) · ADI_NiMo_270 (x1000)

Fig. 8. Microstructure of the ADI_NiMo series ductile irons; etched state (Nital 2%)

ADI_NiCu_370 (x300) · ADI_NiCu_330 (x300) · ADI_NiCu_270 (x300)

ADI_NiCu_370 (x1000) · ADI_NiCu_330 (x1000) · ADI_NiCu_270 (x1000)

Fig. 9. Microstructure of the ADI_NiCu series ductile irons; etched state (Nital 2%)

34CrNiMo6 (H) (x500) GS40CrMo4 (H) (x500) **L**35HGS (H) (x500)
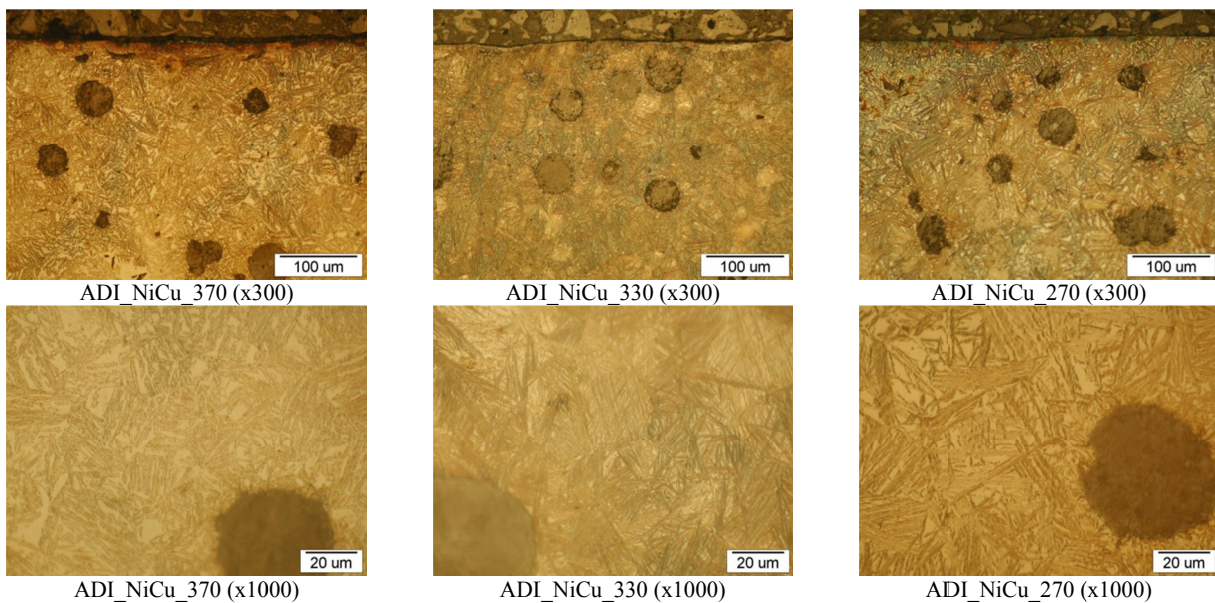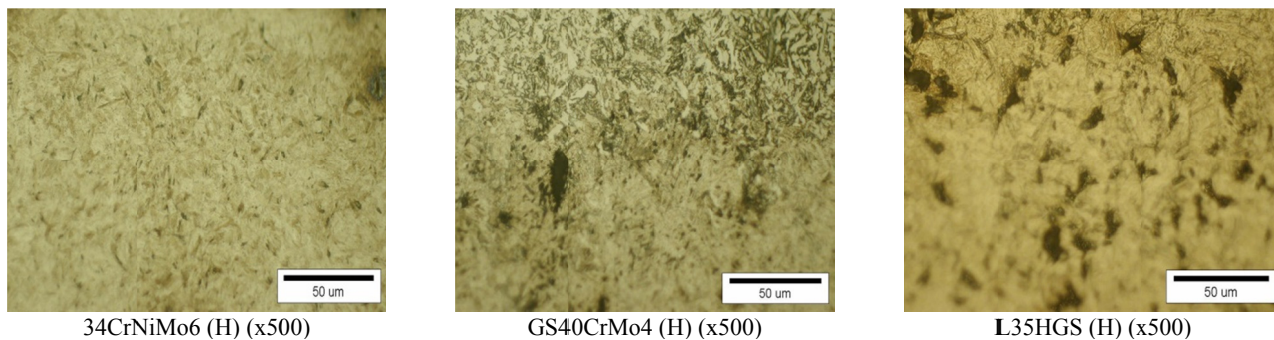
Fig. 10. Microstructure of the 34CrNiMo6 (H) steel as well as the GS40CrMo4 (H) and L35HGS (H) cast steels; etched state (Nital 2%)
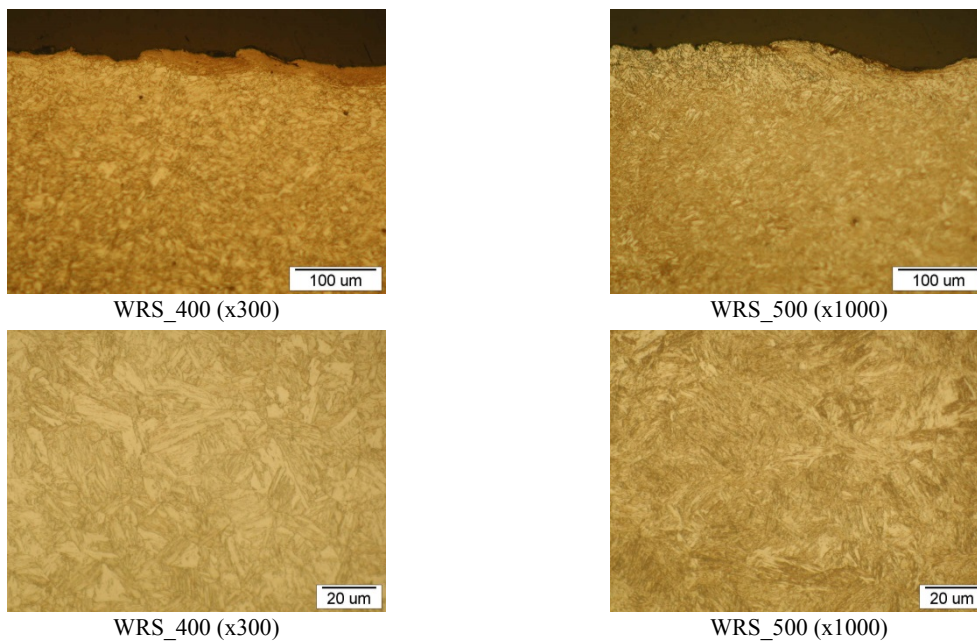

WRS_400 (x300) WRS_500 (x1000)

WRS_400 (x300) WRS_500 (x1000)

Fig. 11. Microstructure of the WRS_400 and WRS_500 steels

(x300) (x1000)
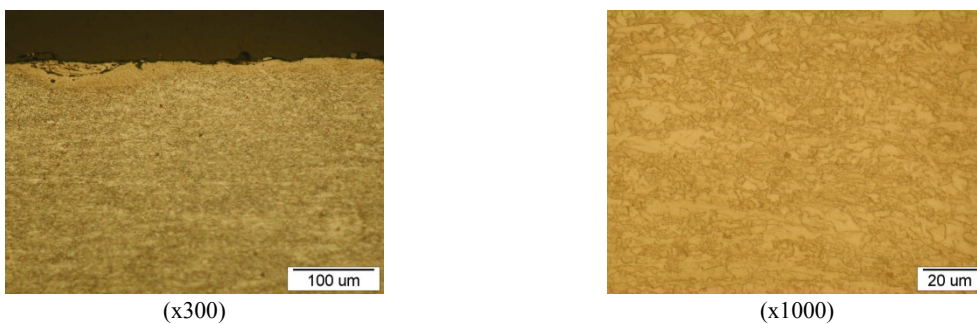
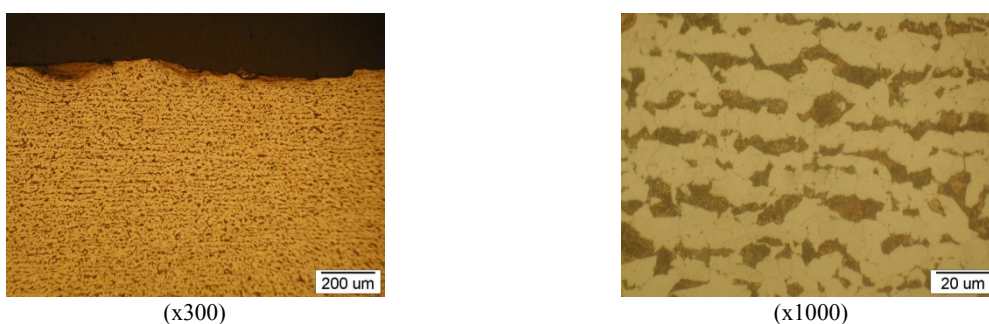Fig. 12. Microstructure of the STEEL_700MC steel

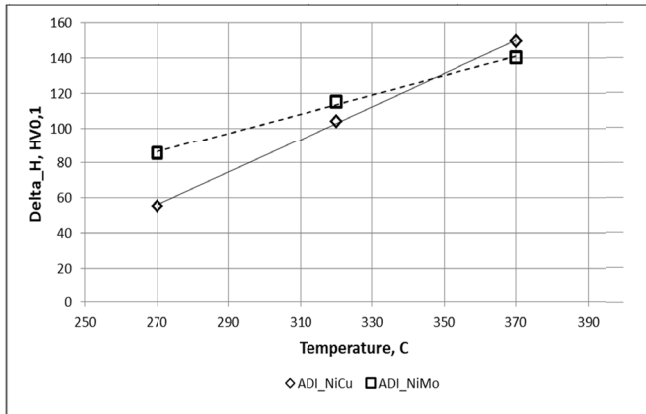(x300) (x1000)

Fig. 13. Microstructure of the S355J2 steel

Fig. 14. The difference in the hardness between the surface and the core (Delta_H) as a function of the isothermal quenching temperature determined for the ADI_NiCu and ADI_NiMo series cast irons
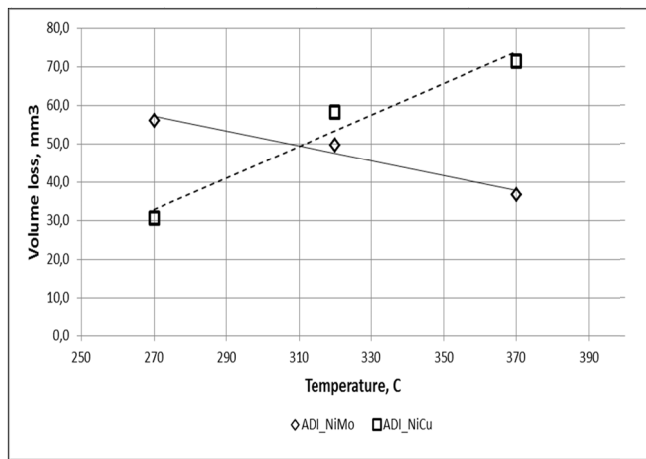

Fig. 15. Values of the volumetric wear as a function of the isothermal quenching temperature determined for the ADI_NiCu and ADI_NiMo series cast irons under a preasure $\sigma = 0.062$ MPa

resistance was 90 min. The author of the study [28] also established, based on a test reproducing the real operating conditions of machine elements, an increase of the linear wear along with an increase of the austenite content in the microstructure, which grew linearly along with an increase in the isothermal quenching temperature. Prasanna et al. [29], on the basis of an erosion test of ADI quenched isothermally for 40 to 200 minutes at temperatures of 320°C and 400°C, made a similar observation: cast iron quenched at a lower temperature had better wear properties. A decrease in the wear along with an increase in the quenching temperature was found only by Wieczorek [28], but the wear tests analysed were carried out in conditions of a strong impact of external dynamic forces on the surface of cast irons.

However, in the wear tests presented in this study, there were no additional external forces, so the dependence observed for the ADI_NiMo cast irons could not be explained by their impact. It seems that the impact resistance may have a certain influence on the wear processes, which was also noted in [30]. However further studies are required in order to explain the dependences observed in the case of austempered cast irons containing Ni and Mo. A comparison is possible only for variants of cast irons

quenched at a temperature of 330°C. In this case similar values of wear are observed, but the variant containing Ni and Mo is more wear resistant. It is also characterized by a higher surface hardness (Fig. 9) and a higher increase in the hardness between the surface and the Delta_H core (Fig. 16).

The range of values of wear parameters determined for the hardened 34CrNiMo6 steel and for the hardened L35HGS cast steel coincides with the range of parameters determined for ADI of all series. The initial hardness of ADI was lower than that of quenched and low-temperature tempered steels and cast steels, however under a load the hardness in the operating surface layer had comparable values (Fig. 5). The GS40CrMo4 cast steel is characterized by a significantly lower wear resistance than austempered cast irons, but in this case it can be stated, based on the measurements of the hardness and examinations of the microstructure, that the heat treatment parameters were not optimal due to the operating requirements applicable in mining.

Häyrynen et al. [7] presented results of abrasive wear tests performed according to the method set forth in the ASTM G132-96 (2001) standard. Fig. 17 shows some results of their studies on hard-wearing steels (the study [7] does not specify mechanical properties of the materials analysed) and ADI. It can be noted that a small group of materials has wear properties comparable to those of cast irons with the ausferritic structure, but a significant group of hard-wearing steels has better wear resistance. Also in the study [31] it was found that surface-hardened steels under conditions of wear in quartz abrasive were characterized by better wear properties than ADI, while cast irons showed a greater resistance to wear than surface hardened hard-wearing cast steels. Gundlach and Janowak [32] presented results of wear tests that also showed comparable wear resistance of hardened steels and ADI, despite a substantial difference in the initial hardness.
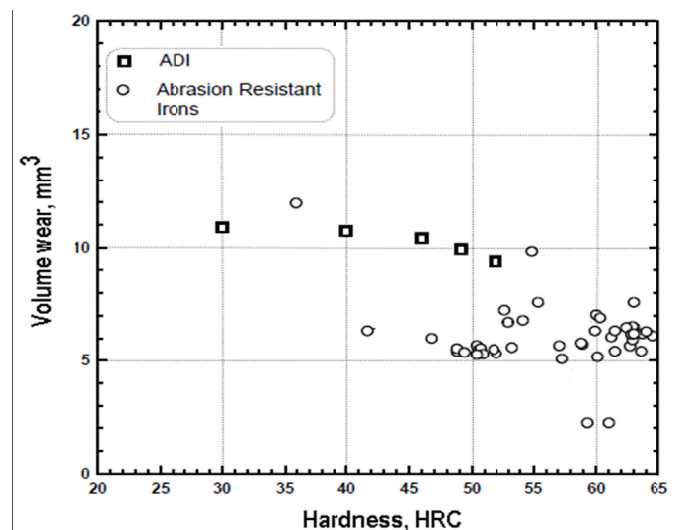

Fig. 16. Results of wear tests concerning ADI and hard-wearing steels, performed according to [7]

Differentiated properties of the ADI in relation to the hardened steels and cast steels may also result from the conditions of wear tests themselves. While the load generated at the point of

contact of three bodies (the sample, the counter-sample and the abrasive material) may cause strengthening of the surface layer as a result of the transformation induced plasticity (TRIP), the forces acting simultaneously may adversely affect the graphite present in the microstructure of cast irons.

The effects of damage to graphite were examined in the study conducted by Chawla et al. [33], in which it was noted that the cracking always began at the contact between graphite nodules and the matrix. It propagated into the material along the austenite and ferrite plates. Al-Ghonamy et al. [34] found an increase in the wear of cast irons along with a reduction in the sphericity of graphite. Tanaka et al. [35] found that cracks occurring at the interface of graphite and the matrix, were caused by a stress concentration in the area where the graphite was present.

Iacoviello et al. [36] examined the mechanism of damage to graphite in nodular cast irons caused by dynamic excitations. They proved the existence of two types of damage manifesting themselves by cracking of graphite nodules inside or on the surface as well as the propagation of cracks in the pearlitic structure starting from the nodular graphite. Wieczorek [28] noted that under the influence of simultaneous action of dynamic forces and abrasive, a strong deformation of graphite nodules and possibly their internal damage took place, which might initiate the crack propagation towards the surface of the samples.

The stresses in the surface layer caused by the load applied lead to a deformation of the graphite nodules. The form of this deformation depends primarily on the microstructure of the ADI matrix and the type of abrasive action on the material.

In the case of cast irons with the structure of lower ausferrite, which is characterised by a high strength and surface hardness as well as a relatively low impact resistance, the degree of the graphite deformation is low. For the variants of ADI_NiMo_270 and ADI_NiCu_270 cast irons (Fig. 17), the graphite occurring in the microstructure shows a small degree of deformation. It grows along with an increase in the austenite content in the microstructure, and thus with an increase in the phase responsible for the plasticity of the material. Also in Fig. 18 it easy to notice a change in the shape of graphite in the case of cast irons with a high content of austenite, i.e. the ADI_NiMo_370 variant, while a characteristic trace after removal of the flattened graphite can be observed for the ADI_NiCu_370 variant.

In the case of wear in the conditions of sliding movement (Fig. 17), the graphite present in the cast iron with the structure of upper ausferrite takes the form of flat lenses located at a slight angle in relation to the surface (this was confirmed also by PourAsiabi et al. [27]). In the case of cracking of a fragment of the material at the base of the cut, the loss is relatively small.

In the cast iron with the structure of upper ausferrite the graphite (Fig. 18) deformed as a result of dynamic strain after the Taylor's test lies flat to the surface [37]. Chinella et al. [38] found a significant deformation of graphite nodules after a ballistic test. In the case of wear tests with sliding-rolling movement of the mating elements [28], graphite deformations are observed also for cast irons with the structure of upper ausferrite, but they are oriented at an angle of approximately 45 degrees. In the case of

cracking of graphite and occurrence of a void, the further cracking of the cut is associated with a significant loss of material. With respect to cast irons with the structure of lower ausferrite, the non-deformed graphite is removed and the cross-section of the resulting void has a shape similar to a triangle, which does not lead to further cracking.

Fig. 17 shows also a view of the surface layer of the 34CrNiMo6 steel as well as the L35HGS and GS40CrMo4 cast steels. A characteristic feature of these materials is the surface with slight traces (below 3 μm) that occurred as a result of the action of the crushed abrasive material.

Hard-wearing hardened steels (WRS_400 and WRS_500) show a lower wear resistance than all the variants of ADI as well as the 34CrNiMo6 steel and the L35HGS cast steel. This can be explained by a lower hardness of the operating surface layer. Only the GS40CrMo4 cast steel shows the wear properties similar to those of the hard-wearing hardened steels.

The 34CrNiMo6 steel as well as the L35HGS and GS40CrMo4 cast steels in the quenched and tempered state showed a worse resistance to abrasive wear as compared with austempered ductile irons and hardened iron alloys. However the difference between them and hard-wearing steels was not large. Such a result should have been expected considering the surface hardness. The materials subjected to quenching and tempering showed better wear properties only in relation to the S355J2 structural steels and the steel subjected to the thermomechanical treatment (STEEL_700MC).

As a result of the tests performed under this study, it was found that values of RWR for the WRS_400 and WRS_500 hard-wearing steels were similar depending on the load and were within the range from 2.7 to 4. No significant increase in the wear resistance caused by the increase in the hardness was found. In the studies [22,23] three various tribological tests were performed to analyse the impact of hard rock grains on the wear. These tests included the S355 steel and three variants of hard-wearing steel with a hardness of 400 and 500 HB. The RWR coefficient for the steel with a hardness of 400 HB was in the range from 1.3 to 2.6, while for 500 HB it ranged from 1.6 to 3.3. The differences between the results obtained in this study and those presented in [22,23] could be caused by the type of the abrasive material used (the corundum abrasive is characterised by a higher hardness and thus a higher aggressiveness).

The ADI had 6 to 14.5 times higher wear resistance than the structural steels. Ghasemi et al. [39] examined the wear of ADI quenched isothermally at the temperatures of 350°C and 315°C as well as forged steel with a ferrite-pearlitic structure (0.4÷0.6 and 0.8÷1.2 Mn). They obtained very similar results – the ADI were 7 to 15 times more resistant to wear than the steel.

5. Conclusions

1. The ADI had a wear resistance comparable with that of the 34CrNiMo6 hardened steel and the L35HGS hardened cast steel.

ADI_NiMo_370   ADI_NiMo_370   ADI_NiMo_330

ADI_NiMo_270   ADI_NiMo_370   ADI_NiMo_330

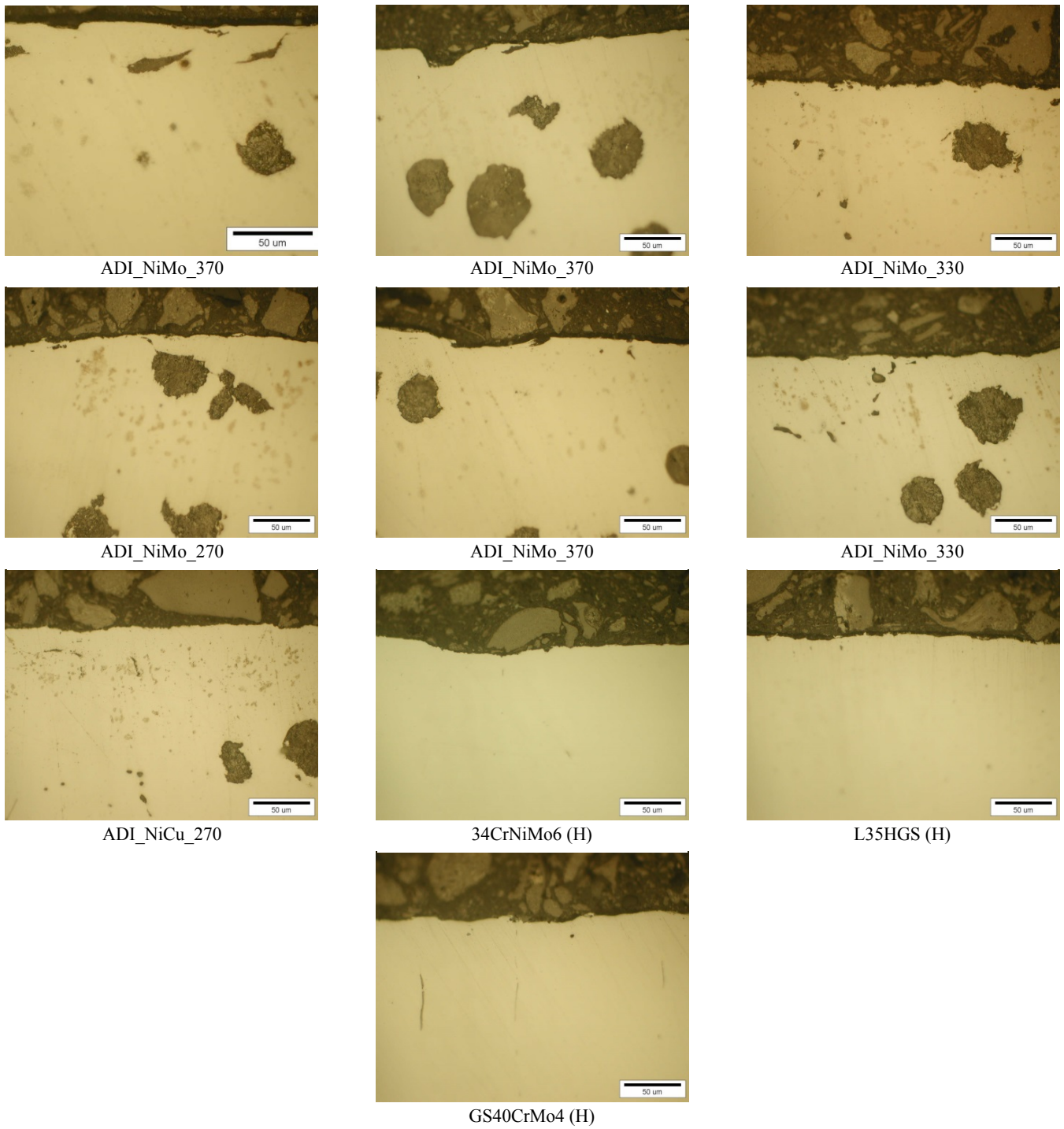ADI_NiCu_270   34CrNiMo6 (H)   L35HGS (H)

GS40CrMo4 (H)

Fig. 17. Surface layer cross-sections of ADI, hardened steels and cast steels at the place of contact; unetched state
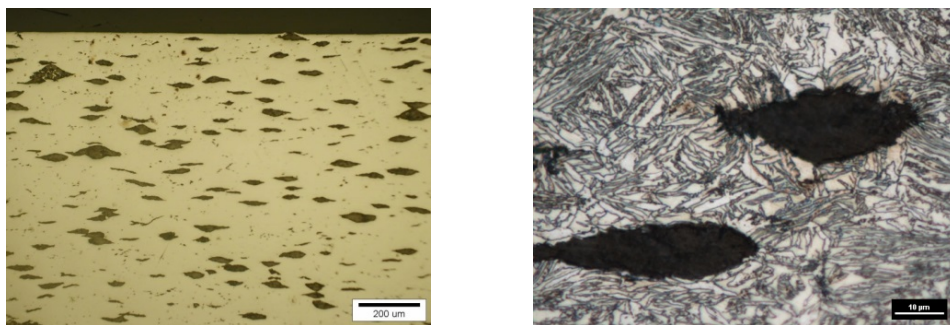

Fig. 18. View of the deformed graphite after the Taylor's test in the cast iron with the structure of upper ausferrite (based on [38])

2. The ADI showed strengthening of the operating surface layer after the wear tests performed.

3. The form of the graphite deformation during the wear tests affects the wear of ADI.

4. Hard-wearing hardened steels showed a lower wear resistance than all the variants of ADI as well as the 34CrNiMo6 steel and the L35HGS cast steel.

5. Structural steels showed a 6 to 14.5 times lower wear resistance than the ADI and the hardened steels and cast steels.

REFERENCES

[1] L. Chybowski, Management Systems in Production Engineering **5**, 10-13 (2012).

[2] B. Skotnicka-Zasadzień, W. Biały, Maintenance and Reliability **3**, 51-55, (2011).

[3] A.N. Wieczorek, Management Systems in Production Engineering, **17**, 28-34, (2015).

[4] R. Burdzik, P. Folęga, B. Łazarz, Z. Stanik, J. Warczek, Archives of Metallurgy and Materials **57** (4), 987-993 (2012).

[5] J.M. Schissler, P. Brenot, J.P. Chobaut, Mater. Sci. Tech. **5**, 71-77, (1987).

[6] A. Owhadi, J. Hedjazi, P. Davami, Mater. Sci. Tech. **14**, 245-250, (1998).

[7] K.L. Hayrynen, J.R. Keough, AFS Transactions **187**, 1-10 (2005).

[8] K.L. Hayrynen, J.R. Keough, G.L. Pioszak, AFS Transactions **129**, 1-15, (2010).

[9] D. Myszka, A.N. Wieczorek, Material Engineering **194**, 332-33 (2013).

[10] D. Myszka, A.N. Wieczorek, Archives of Metallurgy and Materials **58**, 967-970 (2013).

[11] M. Bahmani, Ph.D. Thessis, University of Manchester (1996).

[12] E.P. Fordyce, C. Allen, Wear **135**, 265-278 (1990).

[13] Kumari U. Ritha, Rao P. Prasad, Journal of Materials Science **44**, 1082-1093 (2009).

[14] M.J. Perez, M.M. Cisneros, H.F. Lopez, Wear **260**, 879-885 (2006).

[15] K. B. Rundman, T. Rouns, W. Dubensky, D. Moore, 2nd Int K. Conf. on Austempered Ductile Iron, Ann Arbor, 157-169 (1986).

[16] S. Shepperson, C. Allen, Wear **139**, 573-583 (1987).

[17] W.S. Zhou, Q.D. Zhou, S.K. Meng, „Abrasion resistance of austempered ductile iron", Cast Metals 6, 69-76 (1993).

[18] J. Zimba, M. Samadani, D. Yu, T. Chandra, E. Navara, D.J. Simbi, Material and Design **25**, 431-438 (2004).

[19] J. Zimba, D.J. Simbi, E. Navara, Cement & Concrete Composites **25**, 643-649 (2003).

[20] N. Ojala, K. Valtonen, M. Kallio, J. Aaltonen, P. Siitonen, V.T. Kuokkala, World Tribology Congress (2013).

[21] N. Ojala, K. Valtonen, V. Heino, M. Kallio, J. Aaltonen, P. Siitonen, V.T. Kuokkala, Wear **317**, 225-232 (2014).

[22] V. Ratia, K. Valtonen, A. Kemppainen, V.T. Kuokkala, Tribology Online 8, 152-161 (2013).

[23] V. Ratia, V. Heino, K. Valtonen, M. Vippola, A. Kemppainen, P. Siitonen, V.T. Kuokkala, Tribologia – Finnish Journal of Tribology **32**, 3-18 (2014).

[24] PN-EN 1564:2012 Standard – Austempered ductile cast irons.

[25] M. Dolipski, A. Wieczorek, Science Conference „Mining of Sustainable Development 2010" , Gliwice, (2010).

[26] W. Zwierzycki, Wyd. IteE, Radom-Poznań, (1998).

[27] H. PourAsiabi, H. PourAsiabi, Materials of International Iron & Steel Symposium, 02-04 April, Karabük, Türkiye, 616-625 (2012).

[28] A.N. Wieczorek, Archives of Metallurgy and Materials **59** (4), 1663-167 (2014).

[29] C. Siddaraju, N.D. Prasanna, M.K. Muralidhara, International Journal of Emerging Technology and Advanced Engineering **3**, 124-130 (2013).

[30] A.N. Wieczorek, Archives of Metallurgy and Materials **59** (4), 1653-1662 (2014).

[31] A.N. Wieczorek, A report POIG.01.04.00-24-100/11, (Report no published) (2014).

[32] R. Gundlach, J. Janowak, Proceedings, 2nd International Conference on Austempered Ductile Iron, Ann Arbor, 23-30 (1986).

[33] V. Chawla, Uma Batra, D. Puri, A. Chawla, Journal of Minerals & Materials Characterization & Engineering **7**, 307-316 (2008).

[34] A.I. Al-Ghonamy, M. Ramadan, N. Fathy, K.M Hafez, A.A. El-Wakil, International Journal of Civil & Environmental Engineering **10**, 1-5 (2010).

[35] Y. Tanaka, Z. Yang, K. Miyamoto, Material Transaction, JIM 6, 1995.

[36] F. Iacoviello, V. Di Coccoa, A. Rossia, M. Cavallini, Procedia Materials Science **3**, 295-300 (2014).

[37] D. Myszka, L. Cybula, A.N. Wieczorek, Archives of Metallurgy and Materials **59**, 1181-1189 (2014).

[38] J.F. Chinella, B. Pothier, M.G.H. Wells, Army Research Labaratory, ARL-TR-1741, August (1998).

[39] M. Heydarzadeh Sohi, H.M. Ghasemi, S. Bali, Comparative Tribological Study of Austempered Ductile Iron and Forged Steel, Conference: Advanced Materials Processing Technology AMPT '01, Madrid (2001).